

# Overcoming blockade in producing doubly-excited dimers by a single intense pulse and their decay

Ph. V. Demekhin,\* K. Gokhberg, G. Jabbari, S. Kopelke, A. I. Kuleff, and L. S. Cederbaum  
*Theoretische Chemie, Physikalisch-Chemisches Institut, Universität Heidelberg,  
Im Neuenheimer Feld 229, D-69120 Heidelberg, Germany*

Excitation of two identical species in a cluster by the absorption of two photons of the same energy is strongly suppressed since the excitation of one subunit blocks the excitation of the other one due to the binding Coulomb interaction. Here, we propose a very efficient way to overcome this blockade in producing doubly-excited homoatomic clusters by a single intense laser pulse. For  $\text{Ne}_2$  it is explicitly demonstrated that the optimal carrier frequency of the pulse is given by half of the energy of the target state, which allows one to doubly excite more than half of the dimers at moderate field intensities. These dimers then undergo ultrafast interatomic decay bringing one Ne to its ground state and ionizing the other one. The reported *ab initio* electron spectra present reliable predictions for future experiments by strong laser pulses.

PACS numbers: 33.20.Xx, 32.80.Hd, 41.60.Cr, 82.50.Kx

Blockade is a general term and encompasses many phenomena in different fields investigated for a long time. Thereby a single particle prevents the flow or excitation of other particles [1]. The first studies [2, 3] were on single-electron tunneling induced by blockade interactions and date back to the late 1960's (see also [4–6]). Later on, blockade phenomena have been intensively studied in different realizations with atomic Rydberg gases, where the long-range inter-atomic dipole-dipole interactions prevent the excitation of two identical atoms by the absorption of two photons of the same energy [7]. The excitation blockade was shown to lead to, e.g., spectral line broadening [8–10], enhancement of Penning ionization [11], and non-Poissonian excitation probability distributions [12, 13]. Recently, blockade in ultracold homoatomic ensembles has attracted considerable attention due to its potential application for quantum information processing [1, 7, 14–17]. It has been shown that the excitation of a single atom in the ensemble can block the excitation of other atoms (even when the atoms are more than  $10 \mu\text{m}$  apart [1]) due to the dipolar shift of the atomic levels, which brings the driving pulse out of resonance.

The effect of excitation blockade in an ensemble of atoms is particularly pronounced when these atoms form a cluster where the excited states are also shifted by the binding interaction. Particularly suitable systems to study the phenomenon are rare-gas clusters since the bonding is relatively weak and the constituents preserve, to a large extent, their atomic character. At the same time, rare-gas clusters are easily amenable to experiments: they can be generated in a wide range of different sizes [18, 19], from a few up to millions of atoms, allowing to study a transformation of electronic properties from an atom to the solid. However, even the first excited states of rare-gas atoms lie in the UV range and cannot be accessed by a single photon with conventional optical lasers utilized in the mentioned above experiments with

cold Rydberg atoms.

The advent of the new generation of light sources, like free electron lasers [20, 21] and high-order harmonic generation setups [22, 23] allow one to produce ultrashort and intense coherent laser pulses of high frequencies. Exposed to very strong high-frequency pulses, clusters may absorb a large number of photons creating differently charged ions [24] even if the energy of a single photon is not sufficient to directly ionize them. At moderate field intensities, however, multiple excitation of the clusters dominates over its direct ionization [25–27]. These multiply-excited states then undergo an energy transfer in a very efficient way to produce differently charged ions. Such ionization mechanisms represent a particular case of the broader class of phenomena, known as interatomic Coulombic decay (ICD) [28], important in various fields ranging from physics to biochemistry [29, 30].

Obviously, the blockade mechanism will strongly influence the efficiency of simultaneous excitation of several identical atoms in a cluster. Here, we investigate how to efficiently produce multiply-excited homoatomic clusters by a single intense laser pulse, and how the energy of several photons deposited on different species of a cluster is then transferred to its rest. In order to illustrate our findings, we concentrate on a show-case example of the double-excitation of  $\text{Ne}_2$  by two photons. On the one hand,  $\text{Ne}_2$  is amenable to accurate quantum calculations, including all processes evoked by the strong pulse, as well as the underlying nuclear dynamics, and on the other hand, this example is of interest to experimentalists by itself. Importantly, it allows for a transparent interpretation of the underlying physics. The present results allow us to draw general conclusions which are valid not only for dimers but also for larger clusters.

For the example chosen the process can be schematically described as follows:



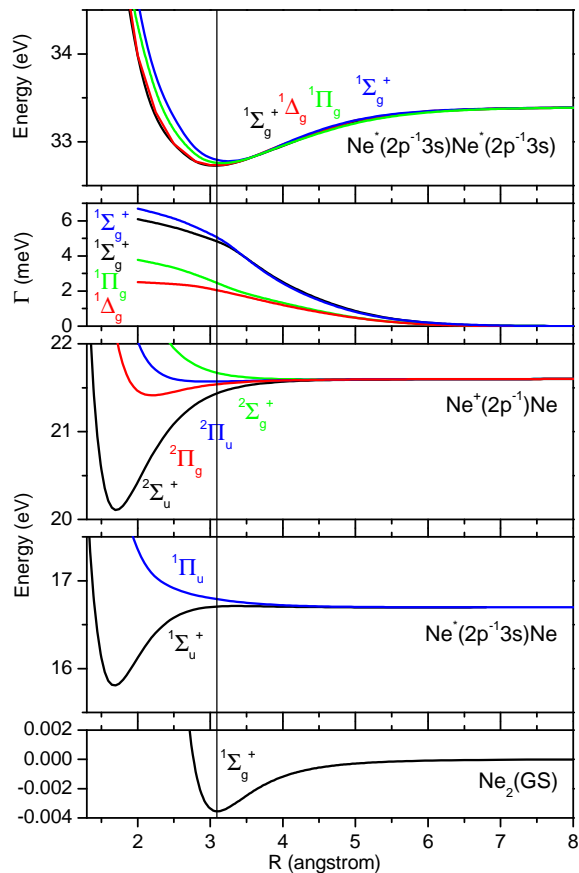


FIG. 1: (Color online) Presently computed *ab initio* PECs and ICD rates of the states relevant to the process (1). These are the  $\text{Ne}_2$  ground state, the ungerade  $\text{Ne}^*(2p^{-1}3s)\text{Ne}$  singly-excited states, the gerade  $\text{Ne}^*(2p^{-1}3s)\text{Ne}^*(2p^{-1}3s)$  doubly-excited states, and the final ionic states  $\text{Ne}^+(2p^{-1})\text{Ne}$ . Total decay rates for each doubly-excited state into all final ionic states are shown in the second panel from the top.

Two photons of energy  $\omega$  excite two Ne atoms in the dimer into their first excited states. These doubly-excited states are located above the first ionization threshold of the dimer and, thus, undergo ICD bringing one Ne to its ground state and ionizing the other one. Fig. 1 depicts *ab initio* potential energy curves (PECs) and total ICD rates for the states relevant to the process (1) which were computed as described in detail in Refs. [31–33]. At the equilibrium internuclear distance ( $R_e = 3.1 \text{ \AA}$ ) of the Ne dimer, resonant population of the singly-excited states requires an energy of about 16.75 eV. The energy difference between the statistically weighted average of the two groups of the singly- and the doubly-excited states computed at 3.1  $\text{ \AA}$  is about 16.03 eV.

How to overcome the enormous blockade of about 0.7 eV and populate the doubly-excited states of the dimer in an efficient way? One can, of course, use two laser pulses with different carrier frequencies of 16.75 and 16.03 eV. Another possibility is to use very short laser pulse of femtosecond or even sub-femtosecond duration,

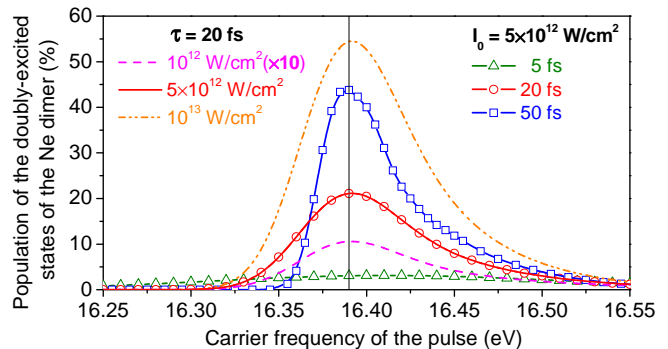


FIG. 2: (Color online) Final population of the doubly-excited states  $\text{Ne}^*(2p^{-1}3s)\text{Ne}^*(2p^{-1}3s)$  as function of the carrier frequency  $\omega$  after the Gaussian pulses of different durations  $\tau$  and peak intensities  $I_0$  have expired. The decay of the doubly-excited states (ICD) has been excluded from the calculations. Open symbols: fixed peak intensity of  $5 \times 10^{12} \text{ W/cm}^2$  and different pulse durations (see right legend). Curves: fixed pulse duration of 20 fs and different peak intensities (see left legend). Note that some results are shown on an enhanced scale as indicated by the  $\times 10$  factor in the legend.

in order to cover the required energy interval. Alternatively, a chirped laser pulse with carrier frequency changing from 16.75 to 16.03 eV can be applied. These strategies are, however, not feasible at present experimental facilities. We suggest an alternative strategy of utilizing a single intense pulse to overcome this blockade.

For this purpose we have performed full quantum mechanical calculations on the double-excitation of the neon dimer by intense laser pulses. In order to compute the process (1) we combined the previously developed theoretical and computational approaches [27, 34–36] to evaluate the excitation and decay processes in intense laser fields. The ensuing non-adiabatic nuclear dynamics has been calculated employing the efficient multiconfiguration time-dependent Hartree (MCTDH) method and code [37, 38]. The values of the electron transition matrix elements for the  $2p \rightarrow 3s$  excitation, the  $3s \rightarrow \varepsilon p$  ionization of the excited states, and the direct two-photon  $2p \rightarrow \varepsilon l$  ionization of Ne atom were taken from the Refs. [39–41]. Calculations were performed for linearly polarized laser pulses  $\mathcal{E}(t) = \mathcal{E}_0 g(t) \cos \omega t$  with Gaussian-shaped envelopes  $g(t) = e^{-t^2/\tau^2}$  of different durations  $\tau$ , carrier frequencies  $\omega$ , and peak intensities  $I_0 = \mathcal{E}_0^2/8\pi\alpha$ .

Fig. 2 depicts the population of the doubly-excited states  $\text{Ne}^*(2p^{-1}3s)\text{Ne}^*(2p^{-1}3s)$  as function of the carrier frequency  $\omega$  after expiration of Gaussian pulses of different durations  $\tau$  and peak intensities  $I_0$ . In order to preserve the population in the doubly-excited states, the ICD transitions from them have been excluded from the calculations. One can see that irrespective of the pulse duration and the peak intensity the optimal carrier frequency of the pulse which allows for a maximal population of the doubly-excited states is equal to

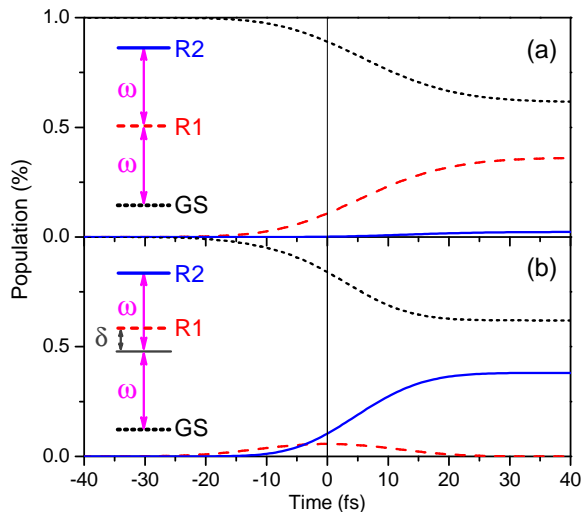


FIG. 3: (Color online) Results of calculations on a three-level model system exposed to a Gaussian pulse of  $\tau = 20$  fs duration and carrier frequency  $\omega = 16.39$  eV. Shown are the populations of the ground state GS (dotted curve), singly-excited state R1 (dashed curve), and doubly-excited state R2 (solid curve) as functions of time. All parameters are taken from the realistic case of  $\text{Ne}_2$  considered here:  $E_{GS} = 0$ ,  $E_{R2} = 2\omega = 32.78$  eV, the dipole transition matrix element for the  $R1 \rightarrow R2$  excitation is  $D = 0.36$  a.u., while the  $GS \rightarrow R1$  excitation is taken to be twice more probable. Panel (a): the state R1 is resonant for the first excitation step,  $E_{R1} = \omega = 16.39$  eV, and the system is predominantly singly-excited after the pulse has expired. Panel (b): the state R1,  $E_{R1} = 16.75$  eV, is off-resonant for the first and for the second excitation steps (detunings are  $\delta = \pm 0.36$  eV). Therefore, R1 serves as a virtual state. The system is essentially only doubly-excited after the pulse has expired. The peak intensities of the pulses are rather moderate and taken to lead to the same level of saturation in both panels (the remaining population of the GS is about 62%). Of course, one needs larger peak intensity ( $7 \times 10^{12}$  W/cm<sup>2</sup>) in the non-resonant case (b) compared to the resonant ( $1.15 \times 10^{11}$  W/cm<sup>2</sup>) case (a).

$\omega = 16.39$  eV. This is exactly the photon energy which is required to access the doubly-excited states by two photons  $E_{2exc} = 2\omega = 32.78$  eV. Another important detail seen from Fig. 2 is that the optimum carrier frequency allows for a very efficient population of the target states (a few tens of percent) at rather moderate peak intensities of about  $10^{13}$  W/cm<sup>2</sup>, although it is detuned far from the resonant transition energies for the first (16.75 eV) and for the second (16.03 eV) excitation steps.

This findings can be rationalized by a simple three-level model. Let us consider a system with a ground electronic level  $|GS\rangle$  of energy 0, an intermediate state  $|R1\rangle$  of energy  $E_{R1}$ , and a target state  $|R2\rangle$  of energy  $E_{R2}$ , which is populated by two photons of energy  $\omega = E_{R2}/2$ . Fig. 3 depicts the populations of these levels by a Gaussian pulse of  $\tau = 20$  fs as a function of time. The electronic properties of the model are indicated in the figure caption and are related to the presently studied

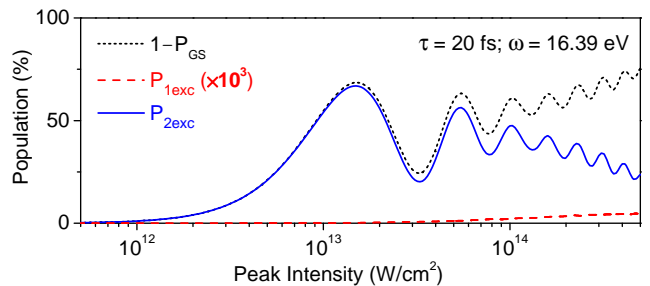


FIG. 4: (Color online) Final populations of the singly- (dashed curve) and doubly-excited (solid curve) states of  $\text{Ne}_2$  after exposure to a Gaussian pulse of 20 fs duration and carrier frequency  $\omega = 16.39$  eV as functions of the peak intensity of the pulse  $I_0$ . The decay of the doubly-excited states (ICD) has been excluded from the calculations, but direct ionizations from the singly- and doubly-excited states which take place during the pulse are accounted for. The dotted curve shows the percentage of the dimers taken out from their ground state by the pulse. Note that the population of the singly-excited states is shown on an enhanced scale as indicated by the  $\times 10^3$  factor in the legend and, thus, is negligible at the considered peak intensities. The difference between solid and dotted curves indicates the impact of the direct ionizations which take away populations from the singly- and doubly-excited states during the pulse.

$\text{Ne}_2$ . In Fig. 3(a), the state  $|R1\rangle$  is resonant for the first excitation step  $E_{R1} = \omega$ . The intense pulse manages to transfer a large fraction of the population from the ground to the first excited state. During the pulse a small fraction of the singly-excited states is further promoted to the final state by the absorption of the second photon of resonant energy. After the pulse has expired the system is predominantly singly-excited.

In Fig. 3(b), both the first and the second excitation steps are off-resonant, but the whole two-photon transition is resonant. In this case the intermediate state  $E_{R1}$  is populated only virtually, and its virtual population is promoted further to the target state  $E_{R2}$  during the pulse duration. Very importantly, after the pulse has expired the final population of the virtual intermediate state is negligibly small, and the system is essentially only doubly-excited. This is due to the energy conservation law which holds for the whole transition  $E_{R2} = 2\omega$ , but does not hold for the first step  $E_{R1} \neq \omega$ . Because of the nuclear dynamics and the large number of electronic states participating, the presently studied  $\text{Ne}_2$  case is much more complicated, but the results shown in Fig. 2 confirm the conclusion drawn. In analogy, one may expect for larger clusters that the target states of several excited atoms are optimally populated if the total energy of several photons fits to the energy of these target states.

Let us now turn back to the process (1). Fig. 4 depicts the final populations of the singly- (dashed curve) and doubly-excited (solid curve) states of  $\text{Ne}_2$  as functions of the peak intensity of the pulse after a Gaussian pulse

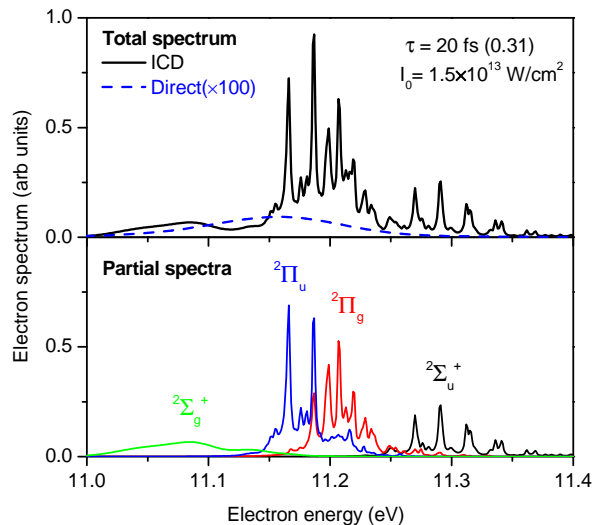


FIG. 5: (Color online) Computed electron spectra after exposure of  $\text{Ne}_2$  to a Gaussian pulse of 20 fs duration, carrier frequency  $\omega = 16.39$  eV, and peak intensity  $1.5 \times 10^{13}$  W/cm $^2$ . Upper panel: Total spectrum. This spectrum is identical with the ICD spectrum because the individual contribution to the spectrum from direct ionization (broken curve) is negligible. After the pulse has expired 31% of the dimers remain in their ground state and 69% are promoted to the doubly-excited states and undergo ICD (see also Fig. 4). Lower panel: The breakup of the spectrum into the contributions of the four final ionic states (see Fig. 1).

with optimal carrier frequency  $\omega = 16.39$  eV and 20 fs duration has expired. The decay of the doubly-excited states (ICD) has been excluded from the calculations, but direct ionizations from the singly- and doubly-excited states which take place during the pulse are accounted for. As was already discussed above, the population of the singly-excited states is almost negligible (note the  $\times 10^3$  factor), and at peak intensities below  $10^{13}$  W/cm $^2$  all the dimers which were taken out from their ground state by the pulse (dotted curve) are promoted to the doubly-excited states. Interestingly, these dimers constitute a big fraction (69% at  $1.5 \times 10^{13}$  W/cm $^2$ ).

At peak intensities above  $10^{13}$  W/cm $^2$  ionization of the dimer starts to play a noticeable role. This is the ionization of the singly-excited states  $\text{Ne}^*(2p^{-1}3s)\text{Ne}$  by a second photon, and also the ionization of the doubly-excited states  $\text{Ne}^*(2p^{-1}3s)\text{Ne}^*(2p^{-1}3s)$  by a third photon. These ‘parasitic’ processes become important at intensities of about  $10^{14}$  W/cm $^2$ , and considerably reduce the ‘desired’ population of the doubly-excited states (see the difference between solid and dotted curves in Fig. 4). We also note that the direct two-photon ionization of the ground state is negligible at the considered peak intensities. The maximal population of the target doubly-excited states by the 20 fs pulse requires the optimal carrier frequency  $\omega = 16.39$  eV and peak intensity of  $I_0 = 1.5 \times 10^{13}$  W/cm $^2$ .

Let us now turn to the decay mechanism of the target states and to resulting electron spectra. The average decay lifetime of the  $\text{Ne}^*(2p^{-1}3s)\text{Ne}^*(2p^{-1}3s)$  states at the equilibrium internuclear distance is around 200 fs (see total decay rates in Fig. 1). Consequently, ICD takes place after the 20 fs pulse has already expired (i.e., in a field-free regime). The total electron spectrum of  $\text{Ne}_2$  exposed to the  $\tau = 20$  fs pulse of carrier frequency  $\omega = 16.39$  eV and peak intensity  $I_0 = 1.5 \times 10^{13}$  W/cm $^2$  is depicted in the upper panel of Fig. 5 by a solid curve. At this field intensity, the ionization of the dimer proceeds entirely via the ICD mechanism, since the individual contribution to the spectrum from the direct ionization (dashed curve shown on an enhanced scale) is negligible. After the pulse has expired, 31% of the dimers remain in their ground state and the rest is promoted to the decaying states. Therefore, the integral intensity of the spectrum amounts to 69%.

Interestingly, the computed total electron spectrum in Fig. 5 exhibits well pronounced resonant structures, which are due to the vibrational levels of the final ionic states  $\text{Ne}^+(2p^{-1})\text{Ne}$ . One can learn about the individual ionization pathways from the lower panel of Fig. 5 where the breakup of the spectrum into the individual contributions of the four final ionic states of different symmetry is depicted. We also mention that these final ionic states are in part weakly bound or even dissociative (see Fig. 1). Following Fig. 1, the high-energy electrons produced via the decays into the  $^2\Sigma_u^+$ ,  $^2\Pi_g$ , and partly into the  $^2\Pi_u$  final ionic states result in the formation of bound singly-charged  $\text{Ne}_2^+$  dimers. The low-energy electrons associated with the decay into the  $^2\Sigma_g^+$  and partly into the  $^2\Pi_u$  ionic states result in the fragmentation of the dimer into a  $\text{Ne}^+$  ion and a Ne atom. For larger clusters, several excited pairs are likely to be present and undergo ICD, and hence fragmentation or Coulomb explosion will rather be the rule. Here, it also helps that the efficiency of the interatomic decay grows with the size of a cluster [42, 43].

In conclusion, it is demonstrated that the blockade of double-excitation of identical atoms in a cluster by the absorption of two photons from the same pulse can be overcome efficiently even for rather long pulses and moderate peak intensities. High-level *ab initio* calculations of the double-excitation of Ne dimers demonstrate that the total energy of the two photons must fit to the energy of the target states, i.e. that the whole double-excitation process is resonant. We suggest that this rule also holds for the multi-photon multiple-excitation of larger clusters. This excitation scheme allows to prepare a large fraction of clusters in multiply-excited states, which then relax via interatomic decay. For  $\text{Ne}_2$  we report *ab initio* electron decay spectra which can directly be compared with experiment. We also note that in molecular clusters the character of the blockade mechanism and the efficient way to overcome it will be modified owing to

the internal degrees of freedom and manifold of participating electronic states. Moreover, the subsequent decay process in molecular clusters is, as a rule, much faster [29, 44]. Investigation of how the energy of several photons is deposited on different subunits in a system and understanding of how this energy is then transferred to the rest of the system is an issue of general importance in the science of intense radiation, and the present study is a first step in this direction.

The research leading to these results has received funding from the ERC under the EU's FP7 (AIG No. 227597) and from the IMPRS at the MPIK, Heidelberg.

---

\* philipp.demekhin@pci.uni-heidelberg.de

- [1] E. Urban, *et al.*, *Nature Phys.* **5**, 110 (2009).  
 [2] I. Giaever and H.R. Zeller, *Phys. Rev. Lett.* **20**, 1504 (1968).  
 [3] H.R. Zeller and I. Giaever, *Phys. Rev.* **181**, 789 (1969).  
 [4] T.A. Fulton and G.J. Dolan, *Phys. Rev. Lett.* **59**, 109 (1987).  
 [5] P.J.M. van Bentum, *et al.*, *Phys. Rev. Lett.* **60**, 369 (1988).  
 [6] M.A. Kastner, *Rev. Mod. Phys.* **64**, 849 (1992).  
 [7] D. Comparat and P. Pillet, *J. Opt. Soc. Am. B* **27**, A208 (2010).  
 [8] J.M. Raimond, *et al.*, *J. Phys. B* **14**, L655 (1981).  
 [9] W.R. Anderson, *et al.*, *Phys. Rev. Lett.* **80**, 249 (1998).  
 [10] I. Mourachko, *et al.*, *Phys. Rev. Lett.* **80**, 253 (1998).  
 [11] A. Reinhard, *et al.*, *Phys. Rev. Lett.* **100**, 123007 (2008).  
 [12] T. Cubel Liebisch, *et al.*, *Phys. Rev. Lett.* **95**, 253002 (2005).  
 [13] A. Reinhard, *et al.*, *Phys. Rev. A* **78**, 060702(R) (2008).  
 [14] D. Jaksch, *et al.*, *Phys. Rev. Lett.* **85**, 2208 (2000).  
 [15] M. D. Lukin, *et al.*, *Phys. Rev. Lett.* **87**, 037901 (2001).  
 [16] K. M. Birnbaum, *et al.*, *Nature* **436**, 87 (2005).  
 [17] A. Gaëtan, *et al.*, *Nature Phys.* **5**, 115 (2009).  
 [18] O. F. Hagena, *Surf. Sci.* **106**, 101 (1981).  
 [19] H. Thomas, *et al.*, *Phys. Rev. Lett.* **108**, 133401 (2012).  
 [20] W. Ackermann, *et al.*, *Nature photonics* **1**, 336 (2007).  
 [21] Home page of FERMI at Elettra in Trieste, Italy, <http://www.elettra.trieste.it/FERMI/>.  
 [22] G. Sansone, *et al.*, *Science* **314**, 443 (2006).  
 [23] E. Goulielmakis, *et al.*, *Science* **320**, 1614 (2008).  
 [24] U. Saalmann, *et al.*, *J. Phys. B* **39**, R39 (2006).  
 [25] T. Laarmann, *et al.*, *Phys. Rev. Lett.* **92**, 143401 (2004).  
 [26] A.I. Kuleff, *et al.*, *Phys. Rev. Lett.* **105**, 043004 (2010).  
 [27] Ph.V. Demekhin, *et al.*, *Phys. Rev. Lett.* **107**, 273002 (2011).  
 [28] L.S. Cederbaum, *et al.*, *Phys. Rev. Lett.* **79**, 4778 (1997).  
 [29] V. Averbukh, *et al.*, *J. Electr. Spectr. Relat. Phen.* **183**, 36 (2011).  
 [30] U. Hergenhahn, *J. Electr. Spectr. Relat. Phen.* **184**, 78 (2011); *Int. J. Radiat. Biology* (2012) in press DOI:10.3109/09553002.2012.698031.  
 [31] A.B. Trofimov and J. Schirmer, *J. Phys. B* **28**, 2299 (1995).  
 [32] V. Averbukh and L.S. Cederbaum, *J. Chem. Phys.* **123**, 204107 (2005).  
 [33] S. Kopelke, *et al.*, *J. Chem. Phys.* **134**, 094107 (2011).  
 [34] Ph.V. Demekhin and L.S. Cederbaum, *Phys. Rev. A* **83**, 023422 (2011).  
 [35] L.S. Cederbaum, *et al.*, *Phys. Rev. Lett.* **106**, 123001 (2011).  
 [36] Ph.V. Demekhin, Y.-C. Chiang, and L.S. Cederbaum, *Phys. Rev. A* **84** (2011) 033417.  
 [37] H.-D. Meyer, *et al.*, *Chem. Phys. Lett.* **165**, 73 (1990).  
 [38] G.A. Worth, M.H. Beck, A. Jäckle, and H.-D. Meyer. The MCTDH Package, see <http://mctdh.uni-hd.de>.  
 [39] W.F. Chan, *et al.*, *Phys. Rev. A* **45**, 1420 (1992).  
 [40] R. Kau, *et al.*, *J. Phys. B* **29**, 5673 (1996).  
 [41] C. McKenna and H.W. van der Hart, *J. Phys. B* **37**, 457 (2004).  
 [42] R. Santra, J. Zobeley, and L.S. Cederbaum, *Phys. Rev. B* **64**, 245104 (2001).  
 [43] G. Öhrwall, *et al.*, *Phys. Rev. Lett.* **93**, 173401 (2004).  
 [44] T. Jahnke, *et al.*, *Nature Physics* **6**, 139 (2010).